Proceedings of the 11th Brazilian Congress of Thermal Sciences and Engineering -- ENCIT 2006
Braz. Soc. of Mechanical Sciences and Engineering -- ABCM, Curitiba, Brazil,- Dec. 5-8, 2006

Paper CIT06-0791

AN EMPIRICAL MODEL TO PREDICT THE MASS FLOW RATE OF SOLIDS IN A HIGH TEMPERATURE CIRCULATING FLUIDIZED BED SYSTEM

Rogério Ishikawa Hory - rogerioh@fem.unicamp.br
Jhon Jairo Ramírez Behainne - jorabe@fem.unicamp.br
Araí Augusta Bernárdez Pécora - arai@fem.unicamp.br
Leonardo Goldstein Jr - leonardo@fem.unicamp.br

Department of Thermal and Fluids Engineering
Faculty of Mechanical Engineering,
State University of Campinas, P.O. Box 6122
13083-970, Campinas, SP, Brazil

Abstract. *A second-order empirical model to predict the mass flow rate of solids recirculating in a pilot scale circulating fluidized bed system (CFB) has been proposed. Tests were performed with quartz sand, 353µm mean diameter, at riser temperatures around 400 ^{o}C, using a L-valve as a recycle device. A central composite design (CCD) based on response surface methodology was programmed. The factors involved were gas fluidization velocity, solids inventory and air mass flow rate injected in the L-valve, and the response was the solids recirculation rate. Experimental runs showed that the solids inventory was the main factor influencing the solids recirculation, followed by the gas fluidization velocity and by the interaction between both factors. Further, it was evidenced that the mass flow rate of air injected in the L-valve had no effect, with a level of confidence of 95%. Results were consistent with CFB loop principles and they were in agreement with the solids flow rate range found in the literature, suggesting that the proposed model can also be applied to the CFB coal combustion process, using quartz sand as inert material and limestone as the SO_2 absorber, in the same experimental system.*

Keywords: *Circulating fluidized bed, L-valve, Solids circulation rate, Central composite design..*

1. Introduction

Circulating fluidized beds (CFB) are utilized by numerous gas–solid contacting processes such as coal combustion, coal gasification and catalytic reactions. Normally, CFB systems work in the fast fluidization regimen, in which the gas superficial velocity into the riser overcomes the mean solids transport velocity (Bai et al., 1993). The main components of a CFB system are the riser, the cyclone, the downcomer (or standpipe) and the solid particles feeding device (Kim and Kim, 2002). Additionally, when operating at high temperatures, a non-mechanical valve, L, J or V type is used to get solids returned from the downcomer to the riser (Arena et al., 1998).

Solids mass flow rate circulating through a CFB system has been recognized as key operational parameter, which affects the mass and heat transfer phenomena inside the riser (Yan, et al., 2005). For instance, in combustion applications, the external solids circulation flux affects the process efficiency, and for this reason, suggested optimal values are in the range of 15 to 90 kg.m^{-2}.s (Davidson, 2000). The literature presents several works related with the mass flux rate of solids in CFB systems, but most have been carried out in cold prototypes (Knowlton and Hirsan, 1978; Weinstein et al., 1983; Reiying, et al., 1985; Matsen, 1988; Kim and Kim, 2002). These studies indicated the superficial fluidization velocity, solids inventory, aeration mass flow rate in the non-mechanical valve and solid particles properties as the most important factors on determining the solids mass flux through the standpipe, and some empirical correlations were proposed. Additionally, Knowlton (1988), Rhodes and Laussmann (1992), and Basu and Cheng (2000) showed that the effect of these parameters on the CFB hydrodynamics can be explained by a loop pressure balance analysis. However, in spite of the information obtained from previous searches, data reported in the literature for a CFB loop with L-type valve driving solids at high temperature are limited (Wang et al. 1995).

In the present work, an experimental study was carried out to determine the mass flux of recirculated solids in a bed of inert material (quartz sand), at a mean riser temperature of 400°C, and to establish the proper level of the main operational parameters for the steady operation of a CFB system. An empirical correlation to predict the external solids mass flux, to be applied in the combustion of a Brazilian coal, with limestone as a SO_2 absorber, was built. A technique for the design of experiments was used to reduce development time and overall cost for the process studied, being also an effective via to learn how systems or processes work (Montgomery, 1997).

2. Experimental

2.1. Apparatus and Material

Figure 1 illustrates the schematic diagram of the experimental assembly, composed by a riser (schedule 40S, AISI 310 stainless steel pipe of 102.26 mm internal diameter and 4,500 mm length), and a downcomer (schedule 40S, AISI 310, stainless steel pipe with 62.8mm internal diameter). The assembly was also composed by a tangential cyclone, a solids sampling valve, a solids feeding device and a L-valve.

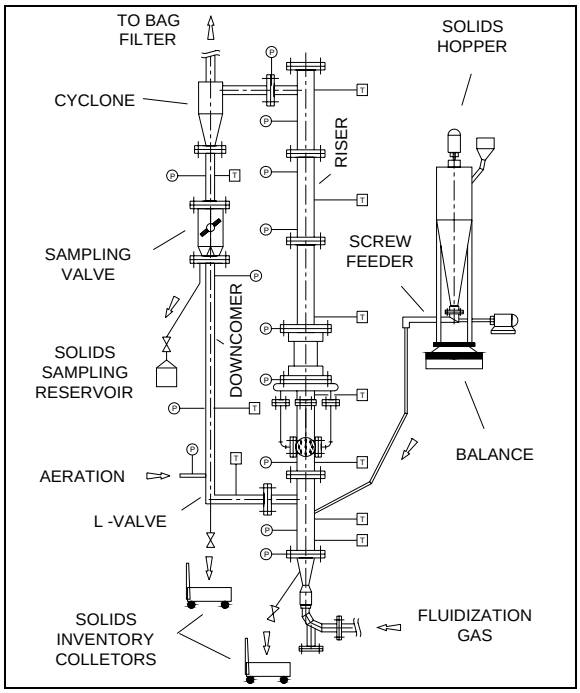

Figure 1 - Experimental CFB System Set-up

Solids are fed by a horizontal screw conveyor positioned at the bottom of a cylindrical hopper and both are positioned over a digital balance. The screw conveyor shaft is connected to a DC motor with rotation controlled by a frequency inverter, which in conjunction with a digital balance controls the solids being fed into the riser. Physical and fluidization properties of quartz sand are shown in Table 1.

Table 1 - Quartz sand properties.

d_p	Distribution size (% mass)						ρ_s	Geldart	u_{mf} [2]	u_{tr} [3]
(μm)	<53[1]	53-105	105-210	210-420	420-840	>840	(kg/m^3)	group	(m/s)	(m/s)
353	0.20	0.48	4.62	57.16	37.48	0.08	2700	B	0.06	5.78

[1] Sieve aperture range (μm); [2] Wen and Yu (1966); [3] Bai *et al.* (1993) – 95.2 kPa, 400°C.

2.2. Experimental Design and Test Procedure

According to Montgomery (1997), conventional experimental procedure, which considers the analysis of only one factor each time is not appropriate for a multi-parameter experiment. Effects of operational parameters, such as the superficial gas velocity, solids inventory and L-valve aeration flow rate, are frequently discussed independently and provided with qualitative descriptions, not informing which parameter is really dominant or how much significant it is. Because the conventional strategy usually jumps to a conclusion merely based on a given operational condition, such a procedure is not sufficient to find out important potential interactions between parameters. On the other hand, when involving many factors, full factorial experiments would not be viable from the viewpoint of time and resources required. Also, they are not indicated to use when factors and response do not follow a linear relationship. In these cases, other alternatives, such as central composite designs are preferable to use.

A central composite design, just as the one shown in Fig. 2, for two factors, consists of a 2^k factorial or "cube" points (coded as –1 and +1), where "*k*" is the number of factors; axial points (also called "star" points) located at (+α ,0), (–α ,0), (0, +α) and (0, –α), and center points positioned at (0,0). The alpha value, which is used to define axial points, corresponds to $\sqrt[4]{2^k}$. In Figure 2, the points represent the experimental runs performed.

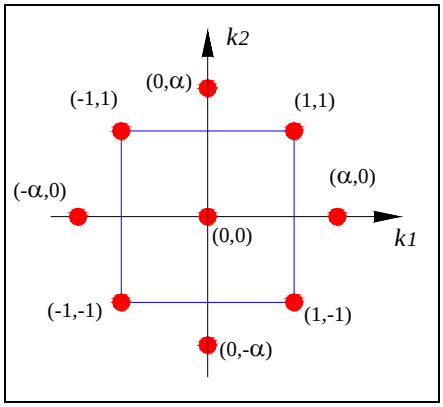

Figure 2 - Central composite design configuration for two factors (k_1, k_2).

The factorial or "cube" portion and center points only serve as a preliminary stage where is possible to fit a first-order (linear) model, but still provide evidence regarding the importance of a second-order contribution or curvature. Adding axial points to the cube portion, an efficient estimation of the quadratic terms for a second-order model is achieved.

In the present work, a central composite design constituted of three controlled factors: solids inventory I_s, fluidization velocity u_f , and aeration mass flow rate in the L-valve $\dot{m}_a$, and one response variable, the mass flow rate of solids through the downcomer G_s, was programmed. Previous runs were done to define the appropriate operational range of the factors involved in the process. For the CFB system analyzed, the -1, 0 and +1 levels of each factor were respectively: 5, 6.5 and 8 kg for the solids inventory, 5, 6 and 7 m/s for the gas fluidization velocity, and 1.4, 2.0 and 2.6 kg/h for the aeration mass rate. Additionally, for the three factors being studied, the alpha value was $\sqrt[4]{2^3} = 1.682$. The sequence of the 17 runs performed, with three runs included at the center point, is presented in Table 2.

Table 2 - Experimental runs.

Run	Factor		
	Solids inventory I_s (kg)	Fluidization velocity u_f (m/s)	Aeration mass rate $\dot{m}_a$ (kg/h)
1	5.0 (-1 level)	5.0 (-1 level)	1.4 (-1 level)
2	5.0 (-1 level)	5.0 (-1 level)	2.6 (+1 level)
3	5.0 (-1 level)	7.0 (+1 level)	1.4 (-1 level)
4	5.0 (-1 level)	7.0 (+1 level)	2.6 (+1 level)
5	8.0 (+1 level)	5.0 (-1 level)	1.4 (-1 level)
6	8.0 (+1 level)	5.0 (-1 level)	2.6 (+1 level)
7	8.0 (+1 level)	7.0 (+1 level)	1.4 (-1 level)
8	8.0 (+1 level)	7.0 (+1 level)	2.6 (+1 level)
9	6.5 (0 level)	6.0 (0 level)	2.0 (0 level)
10	6.5 (0 level)	6.0 (0 level)	2.0 (0 level)
11	6.5 (0 level)	6.0 (0 level)	2.0 (0 level)
12	6.5 (0 level)	6.0 (0 level)	3.0 (+1.682 level)
13	6.5 (0 level)	6.0 (0 level)	1.0 (-1.682 level)
14	4,0 (-1.682 level)	6.0 (0 level)	2.0 (0 level)
15	6.5 (0 level)	4,3 (-1.682 level)	2.0 (0 level)
16	6.5 (0 level)	7,7 (+1.682 level)	2.0 (0 level)
17	9,0 (+1.682 level)	6.0 (0 level)	2.0 (0 level)

Fluidization air was provided by a roots blower. The air was heated in an electrical heater up to 200°C, and next by a petroleum gas burning heater, up to 650°C. Gas flow rate was measured by an orifice plate. Heated gas flowed through the riser during thirty minutes before solids were fed into the system. Just after the entire inventory was loaded, aeration of the L-valve started. The solids recirculation was confirmed by monitoring the pressure and temperature profiles of the system. Steady state was assumed to exist when the mean riser temperature stayed at 400±20°C during thirty minutes. Three solids samples were collected by diverting the particles during periods of 5, 10 and 20s. Solids were re-introduced into the system after sampling, so that the variation of the solids inventory was no more than ± 5% of the initial value.

3. Results and Analysis

Table 3 shows the average solids mass flow rate, G_s, obtained experimentally with the different sampling times (5s, 10s and 20s). An analysis of these results is presented next.

Table 3 - Solids mass flow rate - Experimental runs.

Run	G_s	Run	G_s
1	1.08	10	21.85
2	2.80	11	26.47
3	2.69	12	26.04
4	4.36	13	25.40
5	19.64	14	0.22
6	21.74	15	7.69
7	39.23	16	27.93
8	40.19	17	35.67
9	24.11	--	--

3.1. Factor Effects on the Recirculated Solids Mass Flow Rate

Pareto's chart, shown in Fig. 3, shows the solids mass flow rate estimated by a full statistical model based on a CCD experiment design, involving linear and quadratic main effects together with two-ways interactions. Results demonstrate that only linear terms have a significant influence of 95% of confidence level on the response for solids inventory, fluidization velocity and its interaction. These effects are positive, indicating that an increment in such values increases the solids mass flow rate.

Figure 3 also shows that the quadratic terms referred to the solids inventory and fluidization velocity were also important and had similar effects on the quantity of particles going down through the downcomer, but with values almost equal to the significant p-value (0.05). In this case, the two weak significant effects were negative, which induced the profile to a curvature, and specifically, to the presence of a maximum value on the response.

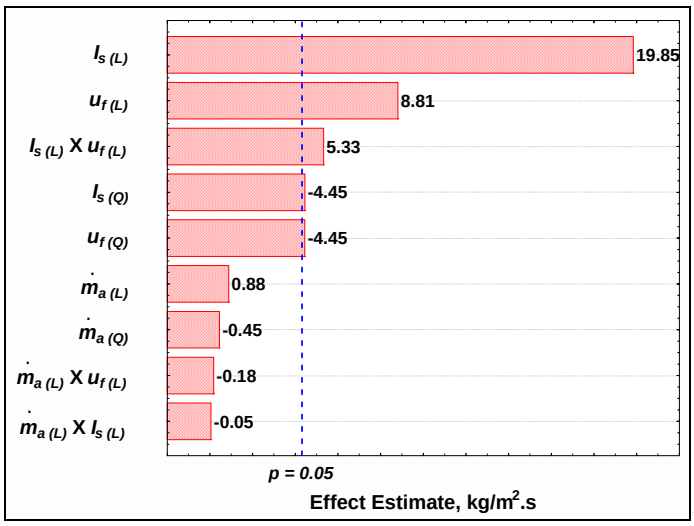

Figure 3 Effect and interaction estimate on the solids mass flow rate (absolute values)-Pareto's chart.
Subscripts: (L) - linear effect; (Q) - quadratic effect.

These results are in agreement with expectations and can be explained based on the three fundamental requirements for a CFB loop operation: mass balance, pressure equilibrium, and relationships between solids mass flow rate, fluidization velocity and riser height (Reiying, et al, 1985; Matsen, 1988, Knowlton, 1988; Rhodes and Lausmann, 1992, Basu and Cheng, 2000).

Mass balance implies that the quantity of solid particles in the fast bed, cyclone, L-valve and downcomer of the CFB loop must be equal to the amount charged into the system, also called solids inventory. Any increase in the quantity of solids in the riser must be accompanied by an equal decrease of the solid particles in the return leg. The solids mass distribution is also associated to the pressure equilibrium around the CFB loop, which basically can be expressed by Eq. (1), where the downcomer pressure drop (Δp_{DC}) is considered as the dependent term:

$$\Delta p_{DC} = \Delta p_R + \Delta p_{CY} + \Delta p_{LV} \tag{1}$$

The riser pressure drop (Δp_R) is determined by the mean concentration of the gas-solid suspension along the riser height, which is proportional to the (G_s/u_f) ratio (Rhodes and Laussmann, 1992). The pressure drop through the cyclone (Δp_{CY}) is proportional to the square of the inlet gas velocity and is usually not dependent on the solids mass flow rate (Matsen, 1988), while the L-valve pressure drop (Δp_{LV}) is proportional to the solids mass flux through it (Arena et al., 1998).

The pressure drop through the downcomer (Δp_{DC}) can be calculated by the modified Ergun equation, assuming that there is a packed bed in the return leg. Such hypothesis is admitted in many CFB configurations (Basu and Cheng, 2000):

$$\Delta p_{DC} = \left[\frac{150.(1-\varepsilon)}{\varepsilon^3} . \frac{\mu_g .(u_0 + u_s)}{(\phi_s .d_p)^2} + \frac{1.75.(1-\varepsilon)^3}{\varepsilon^3} . \frac{\rho_g .(u_0 + u_s)^2}{\phi_s .d_p} \right] .L_{PB} \tag{2}$$

3.1.1. Solids Inventory Effect

Considering the aspects above detailed, the experimental results were as expected. When the solids inventory was increased from 5 to 8 kg, maintained constant both the fluidization velocity and the L-valve aeration mass flow rate, the mass of solids in the CFB zones increased proportionally. As shown in Fig. 3, an average effect estimate of 19.85 kg/m^2.s on the G_s value is attributed to the isolated variation of I_s in the experimental range tested.

The addition of mass in the riser implied in increased solids concentration and higher bed density at the bottom of the column, to preserve the pressure balance around the loop. Consequently, higher solids mass flux through the downcomer should be obtained. For the specific levels analyzed in the experiments and the used CFB configuration, the solids inventory was the more important factor affecting the solids mass flux in the downcomer.

3.1.2 Superficial Fluidization Velocity Effect

Experimental results showed that the fluidization velocity also has a significant effect on the solids mass flux. Figure 3 shows an average effect estimate of 8.81 kg/m^2.s on G_s caused only by the variation of u_f. From Fig. 3 also was evident that, for the range of factors analyzed, the effect caused by I_s was more than twice the one due to u_f.

For higher gas fluidization velocities it is expected that particle concentration at the top of the riser and the void fraction at the bottom of the column increase, due to the higher carrying capacity of the fluidization gas. However, a more detailed analysis must be done concerning the pressure balance, in order to know the magnitude of such effect. When the gas fluidization velocity and the solids inventory increase, while the aeration mass flow rate in the L-valve is maintained constant, a larger mass of particles is transferred from the riser to the downcomer and a higher packed bed is created in the return leg. Consequently, the solids hold up in the fast bed column tends to be continuously reduced if no more particles are transferred by the L-valve to the riser. In fact, for a CFB loop under such conditions, the increase of the solids mass flux going through the valve occurs due to a higher proportion of the aeration gas being forced through the L-valve horizontal leg, induced by the increase on the volumetric concentration of solid particles at the standpipe above the aeration point.

3.1.3 Aeration Mass Flow Rate Effect

The results showed that the air mass flow rate injected in the L-valve had no significant effect on the solids mass flux at 95% of confidence level. As can be seen in Fig. 3, a weak effect of 0.88 kg/m^2.s on G_s was due to $\dot{m}_a$ variations. Apparently such result contradicts the expected behavior of an L-valve, considering this factor is normally used to control the solids flow rate in CFB systems (Arena et al., 1998).

However, Knowlton (1988) suggested that an L-valve can also work in an automatic mode in which, an increase in the aeration mass flow rate, does not necessarily produce a positive variation of the solids flux, because the packed bed localized above the aeration point becomes fluidized. In this circumstance, the downcomer pressure loss attains its maximum value, and therefore, a further pressure drop in the return column, induced by increasing the solids mass flux passing through both the L-valve (below aeration point) and the riser, can not be achieved anymore.

3.2 Empirical Model

A second-order empirical model was proposed, based on the results obtained, to predict the external solids mass flux. Equation (3) expresses the fitted compact model, involving only the most significant factors, u_f, I_s, and their interactions in the tests.

$$G_s = -111.386 + 21.624u_f + 8.326I_s + 2.906u_f.I_s - 2.919u_f^2 - 1{,}342.I_s^2 \qquad R^2 = 0.967 \qquad (3)$$

for $4.0 \text{ kg} \le I_s \le 9.0 \text{ kg}$; $4.3 \text{ m/s} \le u_f \le 7.7 \text{ m/s}$; and $1.0 \text{ kg/h} \le \dot{m}_a \le 3.0 \text{ kg/h}$

The associated response surface of Eq. (3) is shown in Fig. 4.

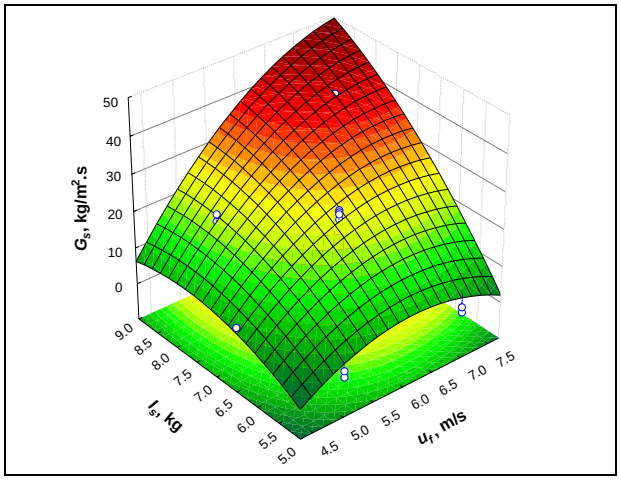

Figure 4 - Response surface of the compact model.

It can be seen that the response surface tends to a maximum value for the solid mass flux, in the analyzed region. Specifically, for the CFB system configuration and operational conditions studied, the maximum mass flux that can be attained is close to 50 kg/m^2.s, when the superficial gas velocity and the solid inventory tend to 8 m/s and 9.0 kg, respectively.

An statistical analysis, including fitting tests and residual studies, was carried out to check the validation of the compact model. The analysis showed that the lack of fit was not significant with 95% of confidence level (p-value=0.407), evidencing the absence of any important deviation in the prediction of the solids flux, as shown in Fig. 5.

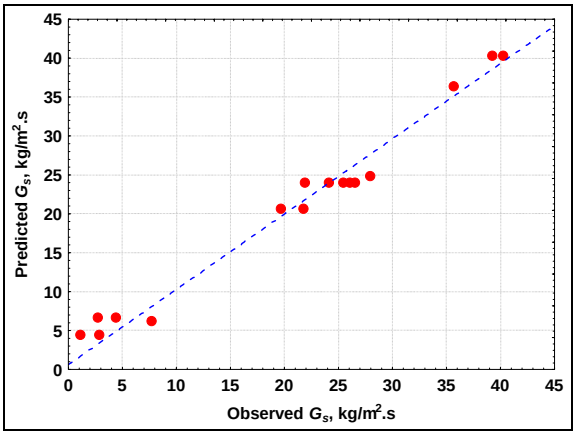

Figure 5 - Observed vs. predicted solids flux for the compact model.

Finally, a residual analysis of the fitted model to predict the solid mass flux was executed. Figure 6 shows that the residuals follow basicaly a normal distribution, with zero mean and constant variance. These results indicate that the proposed second-order correlation is satisfactory.

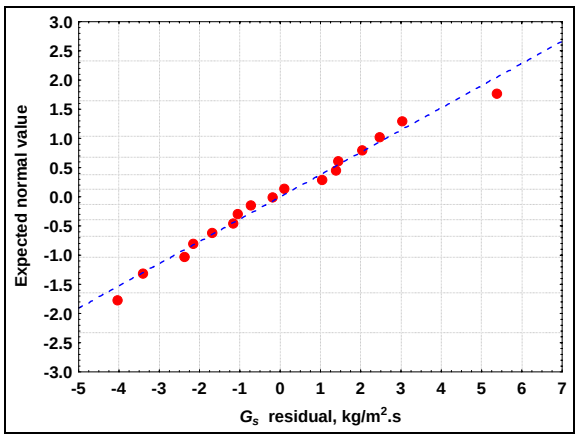

Figure 6 - Expected normal values vs. solids mass flux residuals
Compact empirical model.

4. Conclusions

The analysis of the experiments showed that the particles mass flux trough the downcomer of a CFB system was mainly affected by the solids inventory and the gas fluidization velocity. On maintaining these operational parameters fixed, it was found that the air mass flow rate injected in the L-valve had no influence on the solids mass flux. Experimental results were in accord with the expected behavior of a CFB loop.

For quartz sand at high temperature, an empirical second-order model was developed, based on the experimental results from a CCD designed program of tests. The response surface obtained suggests that the solids mass flux in a CFB system tends to attain a maximum value.

Although the empirical model proposed gave a rough estimate of the particle mass flux level for the several solids inventories and gas fluidization velocity combinations, it may be considered an useful correlation, that can be used in studying the combustion of a Brazilian coal in the specific CFB system used, with quartz sand as the inert material.

As a final remark, one can say that the results were satisfactory and relevant, given the complexity of the process and that fewer experimental runs had to be carried out.

5. Acknowledgement

The authors are grateful to CAPES and CNPq concerning the students scholarships and to FAPESP (Process 05/56621-7) for the financial support.

Nomenclature

d_p	Mean Sauter particle diameter (m)
G_s	Solids mass flow rate based on the cross-section of downcomer (kg/m^2.s)
I_s	Solids inventory (kg)
L_{PB}	Packed bed height at downcomer (m)
$\dot{m}_a$	Air mass flow rate (kg/h)
P	Statistical significant level (-)
R	Correlation coefficient (-)
u_f	Superficial gas velocity in the riser (m/s)
u_{mf}	Minimum fluidization velocity (m/s)
u_o	Superficial gas velocity in the packed bed (m/s)
u_s	Solid particles velocity in the packed bed (Pa)
u_{tr}	Transport velocity (m/s)
ρ_g	Gas density (kg/m^3)
μ_g	Gas viscosity (kg/m.s)
Δp_{CY}	Pressure drop across cyclone (Pa)

Δp_{DC}	Pressure drop across downcomer (Pa)
Δp_{LV}	Pressure drop across L-valve (Pa)
Δp_{R}	Pressure drop across riser (Pa)
ρ_s	Solid particles density (kg/m^3)
Φ_s	Particle sphericity (-)
ε	Voidage in the packed bed (-)

6. References

Arena, U., Langeli, C.B., Cammarota, A., 1998, "L-valve Behavior with Solids of Different Size and Density", Powder Technology, Vol. 98, pp. 231–240.

Bai, D., Jin, Y., Yu, Z., 1993, "Flow Regimes in Circulating Fluidized Beds", Chemical Engineering Technology, Vol. 16, pp. 307–313.

Basu, P., Cheng, L., 2000, "An Analysis of Loop Seal Operations in a Circulating Fluidized Bed", Transactions of the Institution of Chemical Engineers, Vol. 78, pp. 991–998.

Davidson, J. F., 2000. "Circulating Fluidized Bed Hydrodynamics", Powder Technology, Vol. 113, pp. 249–260.

Kim, S.W, Kim, S.D., 2002, "Effects of Particle Properties on Solids Recycle in Loop-seal of a Circulating Fluidized Bed", Powder Technology, Vol. 124, pp. 76–84.

Knowlton, T. M., 1988, "Non-mechanical Solids Feed and Recycle Devices for Circulating Fluidized Beds", Proceedings of the Second International Conference on Circulating Fluidized Beds, Compiègne, France, pp. 31–41.

Knowlton, T. M., Hirsan, I., 1978, "L-valves Characterized for Solids Flow", Hydrocarbon Processing, Vol. 57, No. 3, pp. 149–156.

Matsen, J.M., 1988, "The Rise and Fall of Recurrent Particles: Hydrodynamics of Circulation", Proceedings of the Second International Conference on Circulating Fluidized Beds, Compiègne, France, pp. 3–11.

Montgomery, D. C., 1997, "Design and Analysis of Experiments", Ed. John Wiley and Sons Inc., New York, USA, 704 p.

Reiying, Z., Dabao, C., Guilin, Y., 1985, "Study on Pressure Drop of Fast Fluidized Bed", Fluidization '85: Science and Technology, Second China-Japan Symposium, Kunming, China, pp. 148–157.

Rhodes, M. J., Laussmann, P., 1992, "A Study of the Pressure Balance Around the Loop of a Circulating Fluidized Bed", The Canadian Journal of Chemical Engineering, Vol. 70, pp. 625–630.

Weinstein, H., Graff, R. A., Meller, M., Shao, M. J., 1983, "The Influence of the Imposed Pressure Drop Across a Fast Fluidized Bed", Fluidization, Kunni, D. and Toei, R. (eds), New York, pp. 299-306.

Wang, X. S., Rhodes, M. J., Gibss, B. M., 1995. "Influence of Temperature on Solids Flux Distribution in a CFB Riser", Chemical Engineering Science, Vol. 50, No. 15, pp. 2441–2447.

Wen, C.Y., Yu, Y. H., 1966, "A Generalized Method for Predicting the Minimum Fluidizing Velocity", American Institute of Chemical Engineers Journal, Vol. 12, pp. 610-612.

Yan, A., Ball, J., Zhu, J., 2005. "Scale-up Effect of Riser Reactors (3) Axial and Radial Solids Flux Distribution and Flow Development", Chemical Engineering Journal, Vol. 109, pp. 97–106.